Differences in the Metal Ion Structure between Sr- and Ca-Prothrombin Fragment 1[†,‡]

T. P. Seshadri, E. Skrzypczak-Jankun, M. Yin, and A. Tulinsky*

Department of Chemistry, Michigan State University, East Lansing, Michigan 48824

Received August 25, 1993; Revised Manuscript Received November 19, 1993[⊛]

ABSTRACT: The structure of Sr-prothrombin fragment 1 has been solved and refined by restrained least-squares methods at 2.5-Å resolution to a crystallographic R value of 0.167. The protein structure is very similar to that of Ca-fragment 1. A polymeric array of five Sr^{2+} ions separated by about 4.0 Å is buried among six γ-carboxyglutamic acid (Gla) residues; three other Sr^{2+} ions interact with other Gla residues and are located further apart. One of these was not found in the Ca-fragment 1 structure. The coordination of the Sr^{2+} ions resembles that of Ca^{2+}, but there are some significant differences between them. The most notable is the lack of water coordination with Sr^{2+} ions and two conformations for Gla 8, which change the coordination of Sr-2 and Sr-3. A hexose moiety of an oligosaccharide was located in the vicinity of Asn101 that was flexibly disordered in Ca-fragment 1. The new Sr^{2+} ion found may be involved in metal ion phospholipid binding interactions along with Sr-1, and Sr-7, Sr-8.

Posttranslational modification of 10 glutamic acid residues near the N-terminus of prothrombin to Gla[1] occurs via a vitamin K-dependent carboxylase (Stenflo & Suttie, 1977). Similar modification also takes place in other blood proenzymes such as factors VII, IX, and X and the proteins C, S, and Z. All 10 Gla residues in prothrombin occur in the Gla domain of fragment 1 (Figure 1) (Fernlund et al., 1975; Howard et al., 1975). The Gla residues are primarily responsible for binding to phospholipid in the presence of Ca^{2+} ions during the activation of prothrombin by factor Xa mediated by factor Va. Optimum activation of prothrombin is achieved by the juxtaposition of these factors on the phospholipid surface. The Gla residues of fragment 1 have been shown to bind other di- and trivalent cations as well (Furie et al., 1976; Bajaj et al., 1976; Nelsestuen et al., 1976; Bloom & Mann, 1978). All the metal ions except Sr^{2+} induce conformational modifications resulting in a structure different from that generated by the Ca^{2+} ions. Some of these fragment 1 derivatives are able to bind to phospholipid, but not in the same manner as Ca-fragment 1 (Nelsestuen et al., 1976), whereas Sr^{2+} ions support coagulation with about 20% of Ca^{2+} ion efficiency in blood clotting assays.

The metal ion binding sites of the Gla domain have been classified into two types from fluorescence, circular dichroism and other studies (Deerfield et al., 1987): (a) higher affinity cooperative cation nonspecific sites and (b) lower affinity Ca^{2+} specific sites. It was also shown unambiguously that Sr^{2+} alone can satisfactorily replace Ca^{2+} in both these roles (Nelsestuen et al., 1976). The observations have been rationalized on the basis of conformation-specific antibody studies (Borowski et al., 1986), which demonstrated two conformational transitions. One transition is not cation specific while the second is selective for Ca^{2+} and Sr^{2+} ions, and only the second transition produces the phospholipid binding structure.

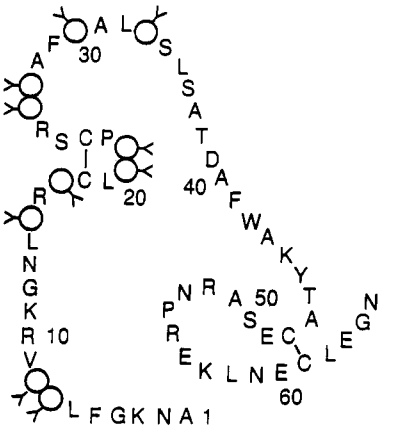

FIGURE 1: Sequence of the Gla domain (1–48) of prothrombin fragment 1. Gla residues, open circles.

The structure of Ca-fragment 1 has been determined crystallographically, where it was shown that seven Ca^{2+} ions bind and interact with Gla residues forming two internal carboxylate surfaces (Soriano-Garcia et al., 1992) and the high-affinity, cooperative Ca^{2+} binding sites (polymeric array of four Ca^{2+} ions separated by about 4.0 Å) were identified that lead to the membrane binding structure. The coordination of the Ca^{2+} ions can be described by distorted polyhedral geometry. Different metal ions binding at the cooperative sites are also the source of a fluorescence quenching event related to a 100° reorientation of Trp42 of the Gla domain. However, different metal ions binding at the sites most likely do not produce the same membrane binding structure.

We report here the structure determination of Sr-prothrombin fragment 1. In agreement with the chemical and biochemical studies, the structure of the protein is similar to that of Ca-fragment 1. The metal ion–protein structure, however, shows significant differences, including two conformations for Gla8, and contains an additional low-affinity Sr^{2+} ion binding site that may be directly related to phospholipid binding. The most notable other difference is that the Sr^{2+} coordination, on the average, is lower than that of

† This work was supported by NIH Grant HL 25942.

‡ The coordinates of Sr-fragment 1 have been deposited in the Brookhaven Protein Data Bank (Access No. 1SPT).

* To whom correspondence should be addressed.

⊛ Abstract published in *Advance ACS Abstracts,* January 15, 1994.

[1] Abbreviations: Gla, γ-carboxyglutamic acid; Gla domain, prothrombin 1-35 or, alternately, prothrombin 1-48 or equivalent in other blood proenzymes; prothrombin fragment 1, prothrombin 1-156; kringle, prothrombin 66-144 or equivalent.

0006-2960/94/0433-1087$04.50/0

Ca^{2+} ions in a very similar structure. This arises from a lack of water coordination of Sr^{2+} ions. Again, as with the Ca-fragment 1 structure, no evidence was found of metal ion binding with the kringle structure of Sr-fragment 1.

MATERIALS AND METHODS

Bovine Sr-prothrombin fragment 1 crystals were grown using the same protocol that produced those of Ca-fragment 1 (Olsson et al., 1982; Soriano-Garcia et al., 1989). They belong to the orthorhombic space group $P2_12_12_1$ with unit cell dimensions a = 39.69(1), b = 54.12(5), and c = 131.17(7) Å that are fairly isomorphous with Ca-fragment 1. The fraction of the unit cell volume occupied by the protein is 40% (V_m = 3.1 Å^3/Da) with one molecule in the asymmetric unit.

X-ray diffraction intensity data were collected with Cu Kα X-rays from a crystal measuring 0.8 × 0.6 × 0.3 mm in size on a Nicolet P3/F four circle diffractometer fitted with a graphite monochromator and sealed X-ray tube operating at 2 kW of power. Intensities were recorded using a wandering Wyckoff step scan procedure (Wyckoff et al., 1967). The intensity data were corrected for absorption (North et al., 1968) and intensity decay with X-ray exposure using procedures similar to those described earlier (Tulinsky et al., 1985). On the basis of a cutoff that was twice the absolute value of the average of the negative intensity measurements for a given 2θ range, 5331 reflections were considered observed, which is 64% of the theoretically accessible 10 366 reflections at 2.8-Å resolution and 51% at 2.5-Å resolution.

A rotation search using the Ca-fragment 1 coordinates (Soriano-Garcia et al., 1992) clearly showed that the fragment 1 molecule is in the same orientation in the Sr-fragment 1 unit cell as expected from unit cell parameters. However, since the unit cell dimension along the c-axis was about 1.5 Å longer in Sr-fragment 1, the structure was positioned more accurately in the unit cell with a translation search. The translation vectors were determined using the program BRUTE (Fujinaga & Read, 1987), which gave a translational shift of 0.1, 0.4, 1.4 Å along xyz in agreement with the difference in the c-axis length. The Sr-fragment 1 structure was refined employing the restrained least-squares procedure implemented by the programs PROFFT (Finzel, 1987) and PROLSQ (Hendrickson, 1985). The refinement was carried out initially with 7.0–2.8-Å data (43 cycles) and subsequently with 7.0–2.5-Å data (90 cycles). In the first refinement stage (Ca-fragment 1 model of 1154 atoms (Soriano-Garcia et al., 1992) with 4267 reflections), R decreased from 30.3 to 21.1%. At the end of this refinement, 60 water molecules and two more Sr^{2+} ions were located, bringing the total of the latter to eight. The structure at the start of 2.5-Å resolution had an R of 19.5%. The refinement continued with addition of more solvent molecules and a 2θ-dependent variable weighting scheme was applied to the observed structure factors in refinement. The final R for 1291 atoms and 4812 reflections converged at 16.7%. The refinement was terminated at this stage as no further reductions in the R index could be accomplished through systematic adjustments of refinement parameters. The final stereochemical restraints used in the refinement of the structure and their deviations from ideal values are given in Table 1. The average thermal parameters for the protein, Sr^{2+} ions, and water oxygen atoms are 38, 38, and 31 Å^2, respectively.

During the course of refinement ($2|F_o| - |F_c|$) and ($|F_o| - |F_c|$) maps were computed several times, and the model was manually fitted to the electron density along with inclusion of solvent molecules. The Sr^{2+} ion–Gla residue interactions were adjusted with aid of the electron and difference density maps to have Sr–O distances in the 2.4–3.0-Å range. These were then utilized as ideal values in restrained refinement but were periodically updated to refined values, which were restrained during the refinement. The occupancies of five Sr^{2+} ions reached unity on refinement; those of the remaining three were 0.64 (Sr-6), 0.65 (Sr-7), and 0.42 (Sr-8) (Figure 2), and their temperature factors varied from 34 to 44 Å^2.

Table 1: Summary of Final Restrained Least-Squares Parameters/Deviations and R Factor Statistics

	target	rms deviations
distances (Å)		
bond lengths	0.020	0.013
bond angles	0.040	0.050
planar 1–4	0.060	0.058
Sr–O	0.030	0.047
planes (Å)		
peptides	0.030	0.016
aromatic groups	0.030	0.016
chiral volumes (Å^3)	0.150	0.170
nonbonded contacts (Å)		
single torsion	0.50	0.25
multiple torsion	0.50	0.33
possible H-bond	0.50	0.33
thermal parameters (Å^2)		
main-chain bond	1.2	0.5
main-chain angle	1.5	0.9
side-chain bond	1.5	0.8
side-chain angle	2.0	1.4
torsion angles (deg)		
planar	3	2
staggered	15	24
orthonormal	20	29
diffraction pattern	A	B
$\sigma(\|F_o\|) = A + B[\sin\theta/\lambda - (1/6)]$	10	−80
$\langle\|\|F_o\| - \|F_c\|\|\rangle$ = 24		
average angle = 117 ± 3.5°		

d_{min} (Å)	no. of reflections	$\sigma(\|F_o\|)$	$\langle\|\|F_o\| - \|F_c\|\|\rangle$	R factor shell	R factor sphere
4.60	1006	15.9	32.5	16.7	16.7
3.95	765	13.8	27.6	15.3	16.1
3.55	733	12.6	24.1	15.2	15.9
3.26	687	11.5	21.0	17.2	17.2
3.02	569	10.6	18.6	18.0	16.3
2.75	573	9.4	16.7	19.5	16.5
2.50	479	8.0	14.9	20.4	16.7

RESULTS AND DISCUSSION

The folding of the polypeptide chain of the Sr-fragment 1 structure illustrated in Figure 2 is essentially the same as that of Ca-fragment 1 (Soriano-Garcia et al., 1992). The root-mean-square (rms) deviation between the two for 435 C_α, C, N pairs is 0.45 Å; removing 75 atoms with deviations > 1σ reduced the rms value to 0.26 Å. The rms deviation for 237 C_α, C, N pairs of the kringle region alone is 0.30 Å, and after removal of 79 deviations > 1σ it reduced to 0.21 Å. The rmsΔ of 301 kringle and 269 Gla domain side chain atoms is 1.0 Å. Five Sr^{2+} ions are located between Gla7–Gla8, Gla17, Gla26–Gla27, and Gla30 (side-chain density for Gla33 is totally absent) that form a polymeric metal ion arrangement (Figures 2 and 3) similar to Ca-fragment 1 and somewhat like that described for Ca^{2+} ion–malonate complexes (Yokomori & Hodgson, 1988). The first four Sr^{2+} ions in the polymeric arrangement are practically in contact with each other with separations not much different from, but consistently about 0.3 Å larger than, those found in the Ca-fragment 1 structure (Table 2). Except for Sr-2, they are in a linear array along an arc buried among the above six Gla residues. The Gla residues 15, 20, and 21 form a separate, looser Sr^{2+}

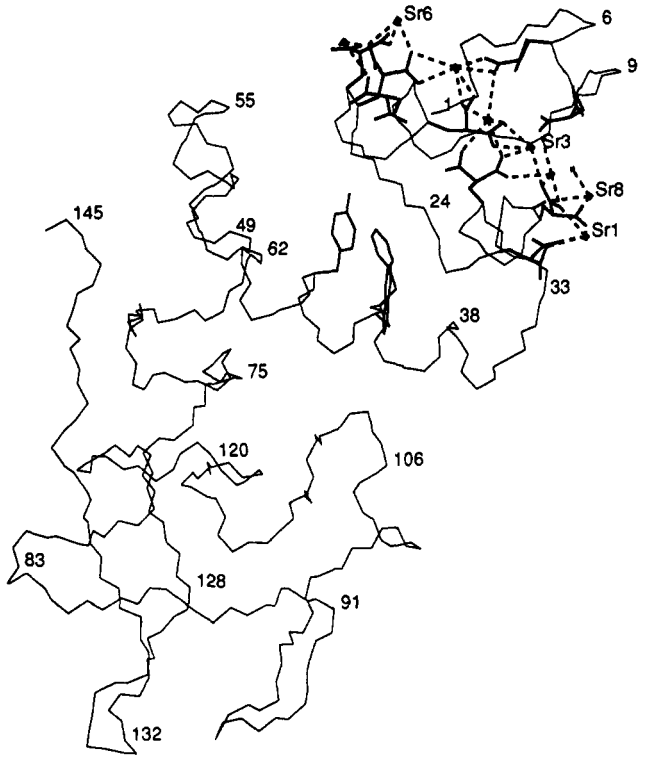

FIGURE 2: The C_α, C, N structure of Sr-fragment 1 and the coordination (dotted) of the Sr^{2+} ions (asterisks) in the Gla domain. Strontium numbering sequential from Sr-1 to Sr-7; Sr-8 adjacent to Sr-1; some amino acid positions numbered in Gla and kringle domains.

ion cluster involving the hexapeptide disulfide loop (Figure 1) of the Gla domain. The last Sr^{2+} ion of the linear array (Sr-5) is 5.1 Å away from Sr-6, with Sr-6 bridging Gla20–Gla21 of the disulfide loop and Sr-7 located between Gla15 and Gla20. The latter two Sr^{2+} ions have a separation of 8.9 Å between them and are exposed to the solvent. The remaining Sr-8 ion is located near Gla30, coordinates a water molecule (W199), and has lower occupancy (0.42 or 15 electrons) but is still highly significant. This cation is not found in the Ca-fragment 1 structure and is at a distance of 7.2 Å from Sr-1

Table 2: Comparison of Closest Distances between Metal Ions in Sr- and Ca-Fragment 1

metal ions	Sr^{2+} d (Å)	Ca^{2+} d (Å)	Δ (Å)
1–8	7.2		
1–2	4.8	4.4	+0.4
2–3	4.3	4.0	+0.3
3–4	4.1	3.8	+0.3
4–5	4.1	3.8	+0.3
5–6	5.1	5.4	−0.3
6–7	8.9	8.5	+0.4

(Figures 2 and 3). Thus, eight Sr^{2+} ions interact with 24 oxygen atoms of 15 out of 18 carboxylate groups of the nine ordered Gla residues of the Gla domain (Table 3) completely burying Sr-2 to Sr-5 (less than 6% solvent accessibility compared to a free ion) (Soriano-Garcia et al., 1992). Equilibrium dialysis measurements using Sr^{90} indicate nine Sr sites, somewhat weaker than Ca^{2+} ion binding, with equilibrium constants varying between 2251 and 113 M^{-1} for eight of them and 10 M^{-1} for one (Huh et al., 1991).

Of the 36 carboxylate oxygen atoms in the Gla domain, 24 make direct contact with Sr^{2+} ions (Table 3), although not all of them are completely in density, most likely because of diffraction effects of neighboring Sr^{2+} ions. Those of Gla17 and Gla27 are completely buried within the domain while all the oxygen atoms of Gla17 and Gla30 interact with Sr^{2+} ions. Moreover, seven of the oxygen atoms are involved in μ-oxo-like bonds bridging two Sr^{2+} ions (Figure 4, Table 4) (Einspahr et al., 1986). There are di-μ-oxo bridges between Sr-3 and Sr-4 and between Sr-4 and Sr-5, but the ones between Sr-1 and Sr-2, and Sr-2 and Sr-3 have a single bridge; the latter is different from Ca-fragment 1, while an additional single μ-oxo bond may exist between Sr-5 and Sr-6, which is only marginal in the Ca-fragment 1 structure (Tables 3 and 4). The spectacular organization of the Sr^{2+} ions and their coordination with Gla residues suggests that they, like Ca^{2+} ions, are responsible for producing the folding transition leading to the phospholipid binding conformation. Thus, the disorder of the Gla domain found in apo-fragment 1 (Park & Tulinsky, 1986; Seshadri et al., 1991) is most likely that of the unfolded chain and not the disorder of a folded structure (Soriano-

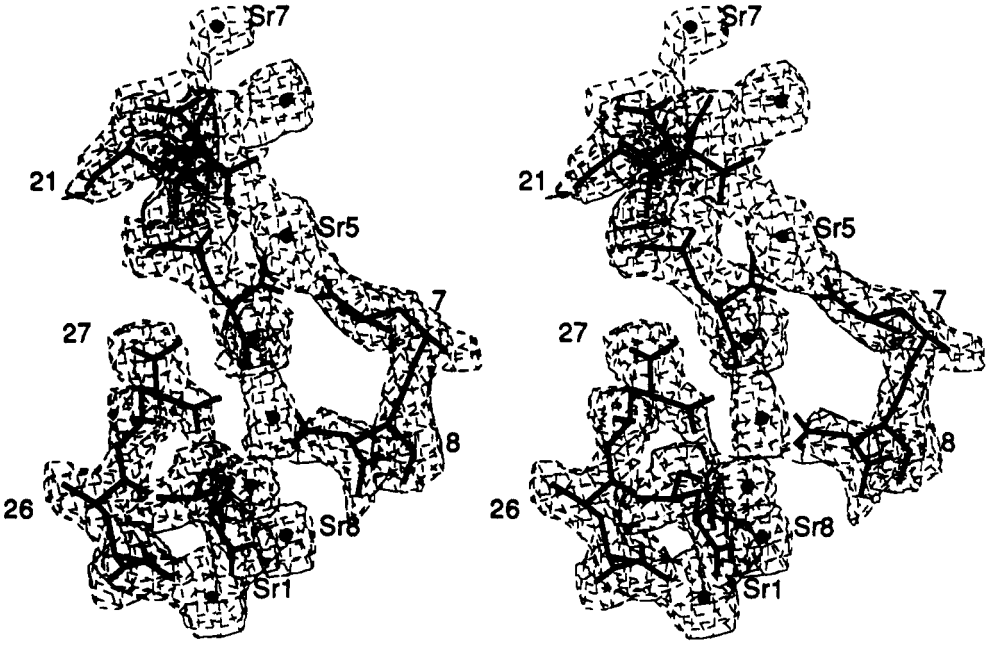

FIGURE 3: Stereoview of $(2|F_o| - |F_c|)$ map contoured at 1σ level showing the Sr^{2+} ions and Gla residues.

Table 3: Comparison of Sr^{2+} and Ca^{2+} Coordination and Sr–O and Ca–O Distances in the Gla Domain[a]

Sr^{2+}/Ca^{2+}	CN	overall type	ligand (residue oxygen)	d (Å)
1	4[4]	m_2	26 O2	2.7 [2.4]
		[m_2]	26 O3	2.7 [2.5]
			30 O1	2.2 [2.4]
			30 O3	2.6[b] [2.5][b]
2	4[6]	u_2b	8 O2	3.5 [2.7][b]
		[ubm(H_2O)]	8 O4	– [2.7]
			27 O2	2.9 [2.8]
			30 O3	2.6[b] [2.4][b]
			30 O4	2.7[b] [2.5][b]
			Ow 266	– [2.7]
3	4[7]	bm	8 O4	– [2.4][b]
		[$u_3b(H_2O)_2$]	17 O1	2.7[b] [2.5][b]
			17 O2	3.2 [2.7]
			27 O1	3.0[b] [2.7][b]
			30 O4	2.8[b] [2.6][b]
			Ow 231	– [2.4]
			Ow 273	– [2.4]
4	6[7]	um_2	7 O1	3.2[b] [2.8][b]
		[u_3m_2(OD1)]	8 O3	– [2.7]
			17 O1	3.3[b] [3.1][b]
			17 O3	2.3[b] [2.0][b]
			27 O1	2.7[b] [2.6][b]
			27 O4	2.8 [2.6]
			Asn2 OD1	3.0 [2.1]
5	6[7]	b_3	7 O1	2.7[b] [2.5][b]
		[$ub_2(H_2O)_2$]	7 O2	2.9 [2.5]
			17 O3	2.6[b] [2.5][b]
			17 O4	3.4 [2.9]
			21 O3	3.2[b] [–]
			21 O4	2.7 [2.8]
			Ow 224	– [3.2]
			Ow 239	– [2.1]
6	3[3]	um	20 O2	2.9 [2.6]
		[um]	21 O1	2.9 [2.7]
			21 O3	2.3 [2.4]
7	3[3]	ub	15 O4	2.8 [2.6]
		[ub]	20 O3	2.4 [2.7]
			20 O4[b]	3.1 [2.4]
8	3[–]	u(CO)(H_2O)	30 O	3.1 [–]
		[–]	30 O2	3.0 [–]
			Ow 199	2.2 [–]
average				2.8 [2.6]
rmsΔ				0.3 [0.3]

[a] CN is the coordination number; OE of Gla residue is listed as O for simplicity preceded by residue number; carboxylate oxygen atoms of independent carboxylate groups of a Gla residue numbered 1,2 and 3,4, respectively; values in brackets are for Ca^{2+} ion structure; u = unidentate, b = bidentate, m = malonate. [b] Participates in the μ-oxo bond between two metal ions.

Garcia et al., 1992). Further, Sr-2 to Sr-5 most likely correspond to the cooperative, tight binding sites recognized from solution studies (Furie et al., 1976; Bajaj et al., 1976; Nelsestuen et al., 1976; Bloom & Mann, 1978; Deerfield et al., 1987) and probably correspond to the Sr^{2+} ion association constants of 2075 (Sr-2), 2251 (Sr-3), 1311 (Sr-4), and 1030 M^{-1} (Sr-5) (Huh et al., 1991); these are the sites that also eventually lead to the production of the native membrane binding structure. The remaining four Sr^{2+} ions probably correspond to the low-affinity sites in agreement with the conclusions reached by the spectroscopic and equilibrium dialysis studies (Sr-1, 740; Sr-6, 309; Sr-7, 286; Sr-8, 113 M^{-1}) (Huh et al., 1991). These sites presumably interact with phosphate groups of a phospholipid surface. The close similarity between the arrangement of Sr^{2+} and Ca^{2+} ions in the Gla region corroborates the earlier suggestion that Sr^{2+} ions can be substituted for Ca^{2+} ions in producing the correct phospholipid binding structure.

The N-terminus of the Gla domain (Figure 2) is embedded in the folded structure and is completely buried. It makes ion

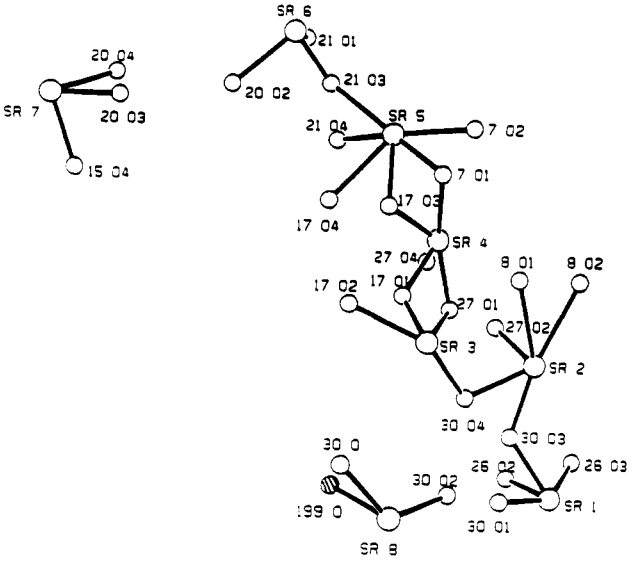

FIGURE 4: Polymeric Sr–O structure of the Gla domain of Sr-fragment 1. Oxygen atoms are from carboxylate groups of Gla residues. Oxygen numbering gives residue number followed by atom number. Water molecule (hatched).

Table 4: Bond Angles of Sr^{2+} Ion–μ-Oxo Bridges

	μ-oxo angle (deg)	di-μ-oxo distance (Å)	sum of angles
Sr-1–30 O3–Sr-2	129		
Sr-2–30 O4–Sr-3	100		
17 O1–Sr-3–27 O1	85	3.9	345
Sr-3–17 O1–Sr-4	87		
17 O1–Sr-4–27 O1	80		
Sr-3–27 O1–Sr-4	93		
7 O1–Sr-4–17 O3	63	2.9	336
Sr-4–7 O1–Sr-5	89		
7 O1–Sr-5–17 O3	63		
Sr-4–17 O3–Sr-5	121		
Sr-5–21 O3–Sr-6	135		

pair interactions with Gla17, Gla21, and Gla27, and it has no area exposed to solvent. The functional role of the Gla domain investigated by site-directed mutagenesis of Gla residues 20 and 21 to aspartic acids in human factor IX (Wolberg et al., 1993) showed that both of these Gla residues are essential for the maintenance of a factor IXa recognizable structure and activation of factor IX to IXa. The participation of Gla21 in hydrogen-bonding interactions with the N-terminal alanine residue and in Sr-5 and Sr-6 coordination amplify these conclusions.

A comparison of the coordination of the Sr^{2+} ions with that of the Ca^{2+} ions (Table 3) shows that there are many similarities but also significant differences between them. The rms deviation between the positions of Sr^{2+} and Ca^{2+} ions is only 0.4 Å, which may be related to their different sizes. However, the Sr–O distances (2.3–3.3 Å) are not very different from those of Ca–O (2.0–3.0 Å). Malonate Ca–O distances hover between 2.2 and 2.6 Å (Einspahr & Bugg, 1981), Ba–O between 2.8 and 2.9 Å (Yokomori et al., 1988), so Sr–O can be expected to be intermediate between the two. The close correspondence could be the result of the increased covalent character of the Sr–O bond. Eight Sr^{2+} ions interact with 33 oxygen atoms, while seven Ca^{2+} ions interact with 37 oxygens, but the coordination around either (Table 3, Figures 2 and 4) does not correspond well with any idealized polyhedra. The coordinations of Sr-6, Sr-7, and Sr-8 are distorted trigonal pyramids, the same as Ca-6 and Ca-7, Sr-1 and Ca-1 approximate a twisted square pyramid, Sr-2 is distorted

Table 5: Dihedral Angles between Gla-Carboxylate Groups Indicating Their Orientations

residue	angle (deg)	residue	angle (deg)
Gla7	71	Gla21	75
Gla8	77	Gla26	47
Gla15	35	Gla27	62
Gla17	59	Gla30	67
Gla20	23		

tetrahedral, while Sr-3 is a flattened square pyramid, Sr-4 is in a dipyramidal geometry, and Sr-5 has incomplete octagonal coordination (Figures 2 and 4). The cooperative sites (Sr-2–Sr-5) have much lower coordination than Ca^{2+} ions (Table 3). The overall coordination of Sr-2 to Sr-5 is 20 and that of Ca^{2+} ions is 27. The difference in coordination of the two is principally due to the lack of water coordination in the case of Sr^{2+} ions although Gla8 has two conformations (about 0.7 and 0.3 occupancy, respectively). The former is most likely related to the larger radius of Sr^{2+}, resulting in decreased polarizing ability. The difference in the enthalpy of hydration of Ca^{2+} and Sr^{2+} ions is about 32 kcal mol^{-1} (Markus, 1985). In addition, there are three di-μ-oxo bonds between Ca-2 and Ca-5, whereas one of the bridges is mono-μ-oxo in Sr-fragment 1 (Sr-2–O–Sr-3, Figure 4). The largest overall difference occurs around the Sr-3 ion (Table 3). Such differences notwithstanding, the Sr^{2+} ion coordination still produces a folded protein structure of the Gla domain that is remarkably similar to that of Ca-fragment 1 (rms$\Delta \sim 0.35$ Å), which also binds to phospholipid in a similar manner (Nelsestuen et al., 1976). The orientations of the carboxylate groups coordinating with the Sr^{2+} ions can be seen in Figure 2, and their dihedral angles are listed in Table 5.

An additional metal binding site has been reported in the kringle region of fragment 1 (Lundblad, 1988; Welsch & Nelsestuen, 1988). This site is in the proximity of carbohydrate-carrying Asn101. In the final stages of refinement, examination of the electron density map in this region revealed a substantial peak that could accommodate a *N*-acetylglucosamine moiety. The *N*-acetyl nitrogen atom forms a hydrogen bond with water 203 but exocyclic oxygens are not involved in hydrogen-bond formation, either with symmetry-related protein molecules or with other water molecules. In contrast, no density was observed in the same region of the Ca-fragment 1 structure. The two nearest peaks in Ca-fragment 1 are located at 3.2 and 4.2 Å from Asn101 and were assigned as water molecules with occupancies 0.6 (B = 31 Å^2) and 0.8 (B = 22 Å^2), respectively. They were not considered as possible cations as there was no semblance of coordination. Thus, neither structure supports evidence for a metal ion binding site near Asn101. This, however, does not exclude such a site since a cation with low occupancy could be mistaken for a water molecule.

Fluorescence quenching of fragment 1 (40%) is reported to occur due to Ca^{2+} binding at neutral pH (Nelsestuen et al., 1976; Prendergast & Mann, 1977). In factor X, the phenomenon was attributed to the alterations in the environment of the lone tryptophan residue of the Gla domain (Nelsestuen et al., 1976). In Sr-fragment 1, just like in the Ca-fragment 1, the conserved aromatic cluster Phe41, Trp42, and Tyr45 interacts with the disulfide bridge of Cys18–Cys23 (Figure 1). The Trp42 in Sr-fragment 1, as in Ca-fragment 1, is rotated by about 90° compared to apo-fragment 1, indicating that both Sr^{2+} and Ca^{2+} ions produce similar conformational changes. Although the fluorescence changes are very comparable, from the present work it is clear that they are produced by fairly different metal ion–protein structures, in agreement with the qualitative nature of such measurements. The fluorescence change undoubtedly signals a conformational change, but considering the radii, charges, and coordination numbers of different metal ions that can produce such changes and the highly intricate structures of Ca- and Sr-fragment 1, the structures resulting from different metal binding are most likely different. This is borne out by the fact that the membrane binding properties of other metal ion Gla domain structures are inferior to those of Ca- and Sr-fragment 1 (Nelsestuen et al., 1976).

Mutagenesis studies have implicated Leu5 of protein C (Leu6 of prothrombin), which is strictly conserved in vitamin K-dependent proteins, as a crucial hydrophobic component of phospholipid binding of the Gla domain (Zhang & Castellino, 1993). Subsequent modeling and solvent accessibility considerations suggested that Ca-1, Ca-2, and Ca-6 are likely involved in the binding to phospholipid (Zhang & Castellino, 1993). Since the Ca-fragment 1 structure did not have a Sr-8 counterpart, the present work would seem to suggest that the phospholipid binding metal ions might better be Sr-1, Sr-8 and Sr-6, Sr-7, located on either side of the Gla domain. Due to their low coordination, the solvent accessible area of these ions is about one-third of that of a free ion (Soriano-Garcia et al., 1992) and all possess a residual positive charge of about $+^1/_2$ to associate with negatively charged phosphate groups of a phospholipid surface. This would still be compatible with the model of insertion of Leu6 and its hydrophobic environment (Phe5, Val9) into the phospholipid surface (Arni et al., 1993; Zhang & Castellino, 1993) and would make the metal ion phospholipid binding interaction more symmetrical. Annexin V behaves in just such a manner as the result of a Ca^{2+} ion induced solvent exposure of a tryptophan in domain 3, which in the presence of phospholipid vesicles is inserted into the membrane in close proximity to the head groups. The Ca^{2+} ion induced conformational changes are supported by fluorescence studies (Meers, 1990; Meers & Mealy, 1993) and crystallography (Concha et al., 1993).

ACKNOWLEDGMENT

We are grateful to Dr. Pappan Padmanabhan for advice and help during the course of this work.

REFERENCES

Arni, R. K., Padmanabhan, K., Padmanabhan, K. P., Wu, T.-P., & Tulinsky, A. (1993) The structure of the non-covalent complex of prothrombin kringle 2 with PPACK-thrombin, *Chem. Phys. Lipids* (in press).

Bajaj, S. P., Nowak, T., & Castellino, F. J. (1976) Interaction of manganese with bovine prothrombin and its thrombin-mediated cleavage products, *J. Biol. Chem. 251*, 6294–6299.

Bloom, J. W., & Mann, K. G. (1978) Metal induced conformational transitions of prothrombin and prothrombin fragment 1, *Biochemistry 17*, 4430–4438.

Borowski, M., Furie, B. C., Bauminger, S., & Furie, B. (1986) Prothrombin requires two sequential metal dependent conformational transitions to bind phospholipid, *J. Biol. Chem. 261*, 14969–14975.

Concha, N. O., Head, J. F., Kaetzel, M. A., Dedman, J. R., & Seaton, B. A. (1993) Rat Annexin V Crystal Structure: Ca^{2+}-Induced Conformational Changes, *Science 261*, 1321–1324.

Deerfield, D. W., Olson, D. L., Berkowitz, P., Koehler, K. A., Pederson, L. G., & Hiskey, R. G. (1987) Relative affinity of Ca(II) and Mg(II) ions for human and bovine prothrombin fragment 1, *Biochem. Biophys. Res. Commun. 144*, 520–527.

Einspahr, H., & Bugg, C. E. (1981) The geometry of calcium-carboxylate interactions in crystalline complexes, *Acta Crystallogr. B37*, 1044–1052.

Einspahr, H., Parks, E. H., Suguna, K., & Subramanian, E. (1986) The crystal structure of pea lectin at 3.0 A resolution, *J. Biol. Chem. 261*, 16518–16527.

Fernlund, P., Stenflo, J., Roepstoff, P., & Thomsen, J. (1975) Vitamin K and the biosynthesis of prothrombin: γ-carboxy glutamic acids, the vitamin K-dependent structures in prothrombin, *J. Biol. Chem. 250*, 6125–6133.

Finzel, B. C. (1987) Incorporation of fast Fourier transforms to speed restrained least-squares refinement of protein structures, *J. Appl. Crystallogr. 20*, 53–55.

Fujinaga, M., & Read, R. J. (1987) Experiences with a new translation-function program, *J. Appl. Crystallogr. 20*, 517–521.

Furie, B. C., Mann, K. G., & Furie, B. (1976) Substitution of lanthanide ions for calcium ions in the activation of bovine prothrombin activated factor X, *J. Biol. Chem. 251*, 3235–3241.

Hendrickson, W. A. (1985) Stereochemically restrained refinement of macromolecular structures, *Methods Enzymol. 115B*, 252–270.

Howard, J. B., Fausch, M. D., & Nelsestuen, G. L. (1975) Amino acid sequence of a vitamin K-dependent Ca^{2+}-binding peptide from bovine prothrombin, *J. Biol. Chem. 250*, 6178–6180.

Huh, N.-W., Berkowitz, P., Hiskey, R. G., & Pedersen, L. G. (1991) Determination of strontium binding to macro molecules, *Anal. Biochem. 198*, 391–393.

Lundblad, R. L. (1988) A hydrophobic site in human prothrombin present in a calcium stabilized conformer, *Biochem. Biophys. Res. Commun. 157*, 295–300.

Markus, Y. (1985) *Ion Solvation*, p 107, Wiley, New York.

Meers, P. (1990) Location of tryptophans in membrane-bound annexins, *Biochemistry 29*, 3325–3330.

Meers, P., & Mealy, T. (1993) Relationship between annexin V tryptophan exposure, calcium and phospholipid binding, *Biochemistry 32*, 5411–5418.

Nelsestuen, G. L., Broderius, M., & Martin, G. (1976) Role of γ-carboxyglutamic acid cation specificity of prothrombin factor X-phospholipid binding, *J. Biol. Chem. 251*, 6886–6893.

North, A. C. T., Phillips, D. C., & Mathews, F. S. (1968) A semi-empirical method for absorption correction, *Acta Crystallogr. 24A*, 351–359.

Olsson, G., Anderson, L., Lindquist, O., Sjolin, L., Magnusson, S., Peterson, T. E., & Sottrup-Jensen, L. (1982) A low resolution model of fragment-1 from bovine prothrombin, *FEBS Lett. 145*, 317–322.

Park, C. H., & Tulinsky, A. (1986) Three dimensional structure of kringle sequence: structure of prothrombin fragment 1, *Biochemistry 25*, 3977–3982.

Prendergast, F. G., & Mann, K. G. (1977) Differentiation of metal induced transitions of prothrombin fragment 1, *J. Biol. Chem. 252*, 840–850.

Seshadri, T. P., Tulinsky, A., Skrzypczak-Jankun, E., & Park, C. H. (1991) Structure of bovine prothrombin fragment 1 refined at 2.25A resolution, *J. Mol. Biol. 220*, 481–494.

Soriano-Garcia, M., Park, C. H., Tulinsky, A., Ravichandran, K. G., & Skrzypczak-Jankun, E. (1989) Structure of Ca^{2+} prothrombin fragment 1 including the conformation of the Gla domain, *Biochemistry 28*, 6805–6810.

Soriano-Garcia, M., Padmanabhan, K., de Vos, A. M., & Tulinsky, A. (1992) The Ca^{2+} ion and membrane binding structure of the Gla domain of Ca-prothrombin fragment 1, *Biochemistry 31*, 2554–2566.

Stenflo, J., & Suttie, J. W. (1977) Vitamin K dependent formation of carboxyglutamic acid, *Annu. Rev. Biochem. 46*, 157–172.

Tulinsky, A., Park, C. H., & Rydel, T. J. (1985) The structure of prothrombin fragment 1 at 3.5 A resolution, *J. Biol. Chem. 260*, 10771–10778.

Welsch, D. J., & Nelsestuen, G. L. (1988) Carbohydrate-linked asparagine 101 of prothrombin contains a metal ion protected acylation site. Acetylation of this site causes loss of metal ion induced protein fluorescence change, *Biochemistry 27*, 4946–4952.

Wolberg, A. S., Cheung, W.-F., Stafford, D. W., & Hamaguchi, N. (1993) Characterization of the functional roles of gamma-carboxyglutamic acid (GLA) residues 20 and 21 in human factor IX, XIV Congress of the International Society of Thrombosis and Haemostasis (July), New York, NY.

Wyckoff, H. W., Doscher, M., Tsernoglou, D., Inagami, T., Johnson, L. N., Hardman, K. D., Allewell, N. M., Kelly, D. M., & Richards, F. M. (1967) Design of a diffractometer and flow cell system for X-ray analysis of crystalline proteins with applications to the crystal chemistry of ribonuclease-S, *J. Mol. Biol. 27*, 563–578.

Yokomori, Y., & Hodgson, D. J. (1988) Calcium binding to γ-carboxyglutamic acid and β-carboxyaspartate residues. Structure of a calcium complex of benzoylmalonic acid, *Inorg. Chem. 27*, 2008–2011.

Yokomori, Y., Flaherty, K. A., & Hodgson, D. J. (1988) Barium binding to γ-carboxyglutamate and β-carboxyaspartate residues, *Inorg. Chem. 27*, 2300–2306.

Zhang, L., & Castellino, F. J. (1993) The hydrophobic component of the binding energy of human coagulation protein C to acidic phospholipid vesicles contains a major contribution from leucine5 in the gamma-carboxyglutamic acid domain, *J. Biol. Chem.* (in press).